

Corrosion Science and Mitigation Strategies: Role of Graphene and Nickel-Graphene Composite Coatings in Next-Generation Protection

Pushp Raj Harsh¹; Ujjwal Prasad¹; S. R. Kumar²; K. Prasad¹

¹University Department of Physics, T. M. Bhagalpur University, Bhagalpur 812007, India

²Department of Applied Science and Humanities, National Institute of Advanced Manufacturing Technology (NIAMT), Hatia, Ranchi 834003, India

Publication Date: 2026/02/12

Abstract: Corrosion is a naturally occurring electrochemical degradation process that imposes severe economic and safety burdens on modern society by reducing the service life of metallic infrastructures in transportation, marine systems, electronics, and energy industries. From a fundamental standpoint, corrosion represents a spontaneous chemical reaction governed by thermodynamic feasibility and electrochemical kinetics, where the driving force is often explained through the Second Law of Thermodynamics and the relative stability of oxidation states in aqueous environments. Accordingly, standard reduction potentials provide an effective framework for predicting the tendency of metallic dissolution and cathodic reduction reactions under practical conditions. This review summarizes the fundamental principles of corrosion, including major corrosion forms such as uniform corrosion, galvanic corrosion, pitting, crevice corrosion, intergranular corrosion, and stress corrosion cracking. A critical discussion is presented on conventional corrosion mitigation strategies, including inhibitors, cathodic protection, alloying, surface passivation, and protective coatings. Particular emphasis is placed on graphene as an emerging corrosion-resistant material due to its high chemical stability, mechanical strength, and exceptional impermeability to aggressive species. The role of graphene as a diffusion barrier is analyzed in terms of defect density, interfacial adhesion, and microstructural integrity. Furthermore, recent progress in nickel-graphene composite coatings is reviewed, highlighting their improved barrier properties, grain refinement effects, enhanced polarization resistance, and suppression of localized corrosion processes. Finally, current challenges and future research directions are outlined, focusing on scalable fabrication, dispersion stability, long-term durability, and the development of multifunctional graphene-enabled anticorrosion coatings for industrial deployment.

Keywords: Corrosion, Graphene, Ni-Graphene, Chemical Vapour Deposition, Electrodeposition, Tafel.

How to Cite: Pushp Raj Harsh; Ujjwal Prasad; S. R. Kumar; K. Prasad (2026) Corrosion Science and Mitigation Strategies: Role of Graphene and Nickel-Graphene Composite Coatings in Next-Generation Protection. *International Journal of Innovative Science and Research Technology*, 11(2), 309-314. <https://doi.org/10.38124/ijisrt/26feb398>

I. INTRODUCTION

Corrosion refers to the chemical or electrochemical interaction between metals or alloys and their surrounding environment, which progressively damages the material and compromises its intended function. Such deterioration not only causes direct economic losses, such as material wastage and leakage of oil or gas, but also contributes to severe indirect consequences, including structural failures of bridges and leakage incidents in nuclear facilities. Previous reports have estimated that the financial impact of corrosion accounts for nearly 5% of the Gross Domestic Product (GDP) in countries such as India, the United States, the United Kingdom, and China.

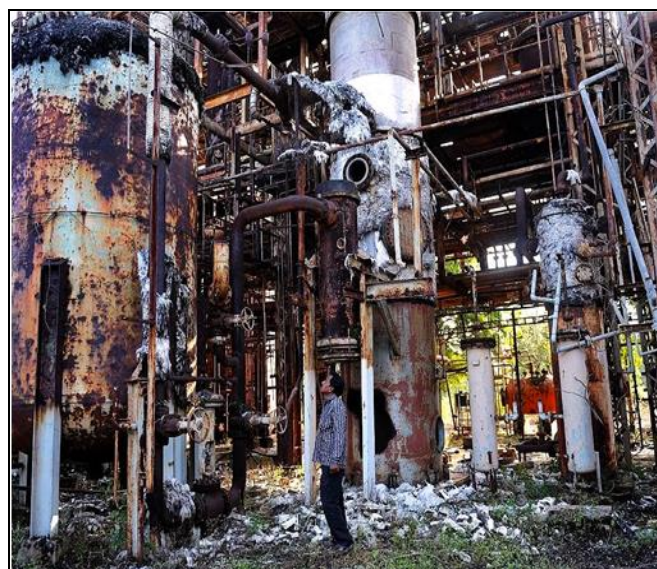




Fig 1 Illustration of Corrosion-Induced Failures Included (a) Severely Degraded Pipelines and (b) the Collapse of a Bridge Structure.

Corrosion typically occurs through reactions between metals and gases or vapours, where both metal oxidation and non-metal reduction take place at the same location. This process is often referred to as the oxidation of metals, as it primarily involves direct chemical interactions between the metal surface and its environment. In contrast, wet corrosion involves electrochemical processes in which the oxidation or dissolution of metals (anodic reaction) and the reduction of non-metals (cathodic reaction) take place at separate sites, coupled by the transfer of electrons to sustain the overall reaction.

Since corrosion is fundamentally a chemical reaction, its feasibility can be explained using the Second Law of Thermodynamics [1], as represented in Equation (1.1):

$$\Delta G = \Delta H - T\Delta S \tag{1.1}$$

Where:

- ΔG represents the change in Gibbs free energy at constant pressure (P) and temperature (T) ($J \cdot mol^{-1}$).
- ΔH denotes the change in enthalpy, i.e., the associated heat change ($J \cdot mol^{-1}$).
- ΔS is the change in entropy ($J \cdot mol^{-1} \cdot K^{-1}$).

- T is the absolute temperature (K)

$$\Delta G = -nFE \tag{1.2}$$

Where:

- n is the number of electrons involved in the electrochemical reaction
- E is the reversible electrode potential at constant P and T (V)
- F is Faraday’s constant ($96,485 C \cdot mol^{-1}$)

In electrochemical corrosion, the overall cell potential ($E_{cathode} - E_{anode}$) must be positive for the reaction to proceed spontaneously. In practice, electrode potentials are referenced against the standard hydrogen electrode (SHE), which is assigned a potential of 0 V and serves as the fundamental scale for comparing redox half-reactions. Representative values are summarized in Table 1 Metals with more negative reduction potentials have a greater tendency to act as anodes, undergoing oxidation while simultaneously enabling the cathodic half-reaction that drives the corrosion of -0.44 V, readily oxidizing in aqueous environments when coupled with the oxygen reduction reaction, which has a potential of +0.40 V.

Since the electrode potential listed in Table 1 corresponds to standard conditions (25 °C, 1 atm, and mol L⁻¹ for aqueous species), they must be adjusted to reflect real experimental conditions. This correction is achieved using the Nernst equation, given as Equation (1.):

$$E = E^\circ - \frac{RT}{nF} \ln \frac{\alpha_{Red}}{\alpha_{Ox}} \tag{1.3}$$

Where:

- E is the actual reduction potential of interest (V)
- E° is the standard reduction potential (V)
- R is the universal gas constant ($8.314 J \cdot K^{-1} \cdot mol^{-1}$)
- T is the absolute temperature (K)
- n represents the number of electrons transferred in the reaction
- α_{Red} is the chemical activity of the reduced species
- α_{Ox} is the chemical activity of the oxidized species.

Table 1 Standard Reduction Potentials of Selected Half-Reactions at 25 °C [17]

Half-Reaction	E° (V)	Half-Reaction	E° (V)
$F_2 + 2e^- \rightarrow 2F^-$	2.87	$O_2 + 2H_2O + 4e^- \rightarrow 4OH^-$	0.40
$Ag^2+ + e^- \rightarrow Ag^+$	1.99	$Cu^{2+} + 2e^- \rightarrow Cu$	0.34
$Co^{3+} + e^- \rightarrow Co^{2+}$	1.82	$Hg_2Cl_2 + 2e^- \rightarrow 2Hg + 2Cl^-$	0.27
$H_2O_2 + 2H^+ + 2e^- \rightarrow 2H_2O$	1.78	$AgCl + e^- \rightarrow Ag + Cl^-$	0.22
$Ce^{4+} + e^- \rightarrow Ce^{3+}$	1.70	$SO_4^{2-} + 4H^+ + 2e^- \rightarrow H_2SO_3 + H_2O$	0.20
$PbO_2 + 4H^+ + SO_4^{2-} + 2e^- \rightarrow PbSO_4 + 2H_2O$	1.69	$Cu^{2+} + e^- \rightarrow Cu^+$	0.16
$MnO_4^- + 4H^+ + 3e^- \rightarrow MnO_2 + 2H_2O$	1.68	$2H^+ + 2e^- \rightarrow H_2$	0.00
$2e^- + 2H^+ + IO_4^- \rightarrow IO_3^- + H_2O$	1.60	$Fe^{3+} + e^- \rightarrow Fe^{2+}$	-0.036
$MnO_4^- + 8H^+ + 5e^- \rightarrow Mn^{2+} + 4H_2O$	1.51	$Pb^{2+} + 2e^- \rightarrow Pb$	-0.13
$Au^{3+} + 3e^- \rightarrow Au$	1.50	$Sn^{2+} + 2e^- \rightarrow Sn$	-0.14

$\text{PbO}_2 + 4\text{H}^+ + 2\text{e}^- \rightarrow \text{Pb}^{2+} + 2\text{H}_2\text{O}$	1.46	$\text{Ni}^{2+} + 2\text{e}^- \rightarrow \text{Ni}$	-0.23
$\text{Cl}_2 + 2\text{e}^- \rightarrow 2\text{Cl}^-$	1.36	$\text{PbSO}_4 + 2\text{e}^- \rightarrow \text{Pb} + \text{SO}_4^{2-}$	-0.35
$\text{Cr}_2\text{O}_7^{2-} + 14\text{H}^+ + 6\text{e}^- \rightarrow 2\text{Cr}^{3+} + 7\text{H}_2\text{O}$	1.33	$\text{Cd}^{2+} + 2\text{e}^- \rightarrow \text{Cd}$	-0.40
$\text{O}_2 + 4\text{H}^+ + 4\text{e}^- \rightarrow 2\text{H}_2\text{O}$	1.23	$\text{Fe}^{2+} + 2\text{e}^- \rightarrow \text{Fe}$	-0.44
$\text{MnO}_2 + 4\text{H}^+ + 2\text{e}^- \rightarrow \text{Mn}^{2+} + 2\text{H}_2\text{O}$	1.21	$\text{Cr}^{3+} + \text{e}^- \rightarrow \text{Cr}^{2+}$	-0.50
$\text{IO}_3^- + 6\text{H}^+ + 5\text{e}^- \rightarrow 1/2\text{I}_2 + 3\text{H}_2\text{O}$	1.20	$\text{Cr}^{3+} + 3\text{e}^- \rightarrow \text{Cr}$	-0.73
$\text{Br}_2 + 2\text{e}^- \rightarrow 2\text{Br}^-$	1.09	$\text{Zn}^{2+} + 2\text{e}^- \rightarrow \text{Zn}$	-0.76
$\text{VO}_2^+ + 2\text{H}^+ + \text{e}^- \rightarrow \text{VO}^{2+} + \text{H}_2\text{O}$	1.00	$2\text{H}_2\text{O} + 2\text{e}^- \rightarrow \text{H}_2 + 2\text{OH}^-$	-0.83
$\text{AuCl}_4^- + 3\text{e}^- \rightarrow \text{Au} + 4\text{Cl}^-$	0.99	$\text{Mn}^{2+} + 2\text{e}^- \rightarrow \text{Mn}$	-1.18
$\text{NO}_3^- + 4\text{H}^+ + 3\text{e}^- \rightarrow \text{NO} + 2\text{H}_2\text{O}$	0.96	$\text{Al}^{3+} + 3\text{e}^- \rightarrow \text{Al}$	-1.66
$\text{ClO}_2 + \text{e}^- \rightarrow \text{ClO}_2^-$	0.954	$\text{H}_2 + 2\text{e}^- \rightarrow 2\text{H}^-$	-2.23
$2\text{Hg}^{2+} + 2\text{e}^- \rightarrow \text{Hg}_2^{2+}$	0.91	$\text{Mg}^{2+} + 2\text{e}^- \rightarrow \text{Mg}$	-2.37
$\text{Ag}^+ + \text{e}^- \rightarrow \text{Ag}$	0.80	$\text{La}^{3+} + 3\text{e}^- \rightarrow \text{La}$	-2.37
$\text{Hg}_2^{2+} + 2\text{e}^- \rightarrow 2\text{Hg}$	0.80	$\text{Na}^+ + \text{e}^- \rightarrow \text{Na}$	-2.71
$\text{Fe}^{3+} + \text{e}^- \rightarrow \text{Fe}^{2+}$	0.77	$\text{Ca}^{2+} + 2\text{e}^- \rightarrow \text{Ca}$	-2.76
$\text{O}_2 + 2\text{H}^+ + 2\text{e}^- \rightarrow \text{H}_2\text{O}_2$	0.68	$\text{Ba}^{2+} + 2\text{e}^- \rightarrow \text{Ba}$	-2.90
$\text{MnO}_4^- + \text{e}^- \rightarrow \text{MnO}_4^{2-}$	0.56	$\text{K}^+ + \text{e}^- \rightarrow \text{K}$	-2.92
$\text{I}_2 + 2\text{e}^- \rightarrow 2\text{I}^-$	0.54	$\text{Li}^+ + \text{e}^- \rightarrow \text{Li}$	-3.05
$\text{Cu}^+ + \text{e}^- \rightarrow \text{Cu}$	0.52		
$\text{ClO}_4^- + 2\text{e}^- \rightarrow \text{ClO}_3^-$	0.67		
$\text{Hg}_2^{2+} + 2\text{e}^- \rightarrow \text{Hg}$	0.85		

II. TYPES OF CORROSION

Corrosion can manifest in several forms, including uniform corrosion, localized corrosion, galvanic corrosion, intergranular corrosion, dealloying, and stress corrosion cracking, among others [2]. In the present thesis, emphasis is placed on discussing the first three types, namely uniform, localized, and galvanic corrosion.

Uniform corrosion, also referred to as general corrosion, is the most prevalent form of corrosion and occurs uniformly across the entire exposed metal surface. Despite being responsible for a significant proportion of overall metal degradation, it is often regarded as a comparatively less dangerous type of corrosion, as its progression is predictable and can be effectively controlled and mitigated.

In contrast, localized corrosion affects specific regions of a metal surface and may occur in forms such as pitting (formation of surface cavities), crevice corrosion (within narrow gaps between adjoining surfaces), and filiform corrosion (beneath coated or painted layers). Compared to uniform corrosion, localized corrosion is considered more determined, as it typically progresses at a faster rate, is more difficult to control, and results in more severe structural damage to metals.

Galvanic corrosion, also known as bimetallic corrosion, is defined by NACE International [3] as the corrosion

associated with the current resulting from an electrical coupling of dissimilar electrodes in an electrolyte. This form of corrosion tends to accelerate pre-existing corrosion processes but can often be mitigated through appropriate design considerations. Fig. 2 illustrates the case of galvanic corrosion between iron and tin, where tin, being more noble, is less prone to corrosion compared to iron. In this system, the oxidation of iron leads to the release of Fe^{2+} ions, which subsequently react with dissolved oxygen in the electrolyte to produce iron hydroxides or oxides that deposit as rust on the surface. The electrons liberated during the oxidation of iron are transferred to tin, facilitated by the potential difference between the two metals. As a result, the tin surface functions as an extensive cathode, significantly enhancing the rate of cathodic oxygen reduction reactions, thereby accelerating the overall corrosion of iron [2, 4].

Metals and alloys serve as essential structural materials across a wide range of industries, making corrosion protection crucial not only for extending the service life of industrial systems and minimizing economic losses but also for mitigating negative environmental and societal consequences, such as pollution and catastrophic failure. Over the years, a variety of corrosion protection strategies have been developed [2]. These approaches include surface pretreatment, application of anticorrosive coating, cathodic and anodic protection techniques, the use of corrosion inhibitors, and the development of corrosion-resistant materials, among others.

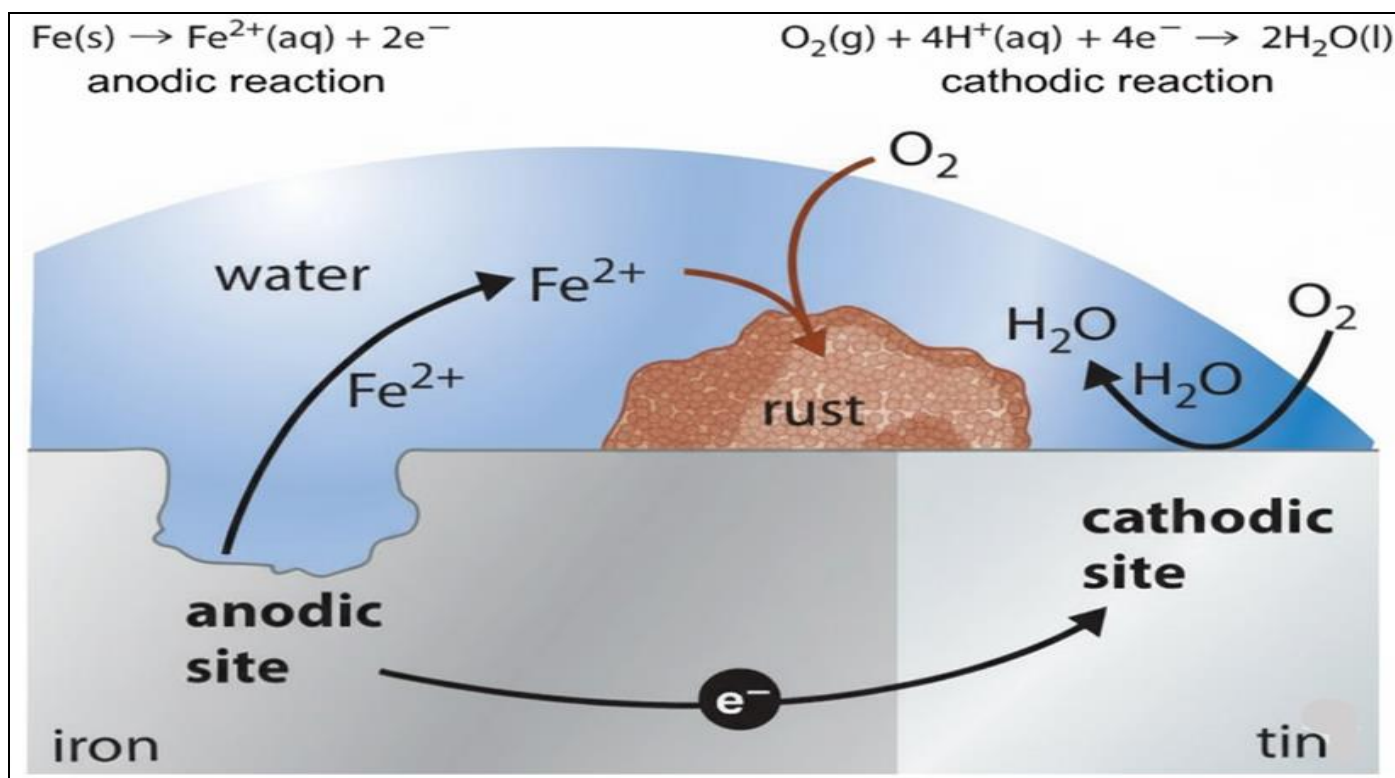


Fig 2 Representation of Galvanic Corrosion Occurring When Iron is Coupled with Tin [4].

Surface treatments are employed to alter the condition, chemical composition, or microstructure of metal surfaces to enhance their stability, with common approaches including plasma ablation and chemical etching [2, 5, 6]. In contrast, corrosion-resistant materials such as stainless steels and titanium alloys are widely used in specialized applications, including deep-sea and aerospace equipment, where high levels of corrosion resistance are required under demanding service conditions [7, 8].

Coatings are among the most widely adopted methods for corrosion protection, and they can be broadly classified into metallic (e.g., noble chromium and sacrificial zinc coatings), inorganic (e.g., zinc silicate and SiO_2 coatings), and organic type (e.g., resins and latexes) [9]. These coatings protect metals through different mechanisms, including barrier action, surface passivation (inhibition), or sacrificial protection (galvanic effect). Anticorrosive coatings are typically designed as multilayer systems, with each layer serving a distinct function. For instance, in marine and aerospace applications, a conventional coating system is composed of three layers: pretreatment, primer, and topcoat [6]. The pretreatment layer, which is in direct contact with the substrate, ensures mechanical or chemical adhesion and prevents direct exposure of the substrate to the environment, thereby delaying coating failure. This layer, also known as the conversion layer, is usually a thin inorganic film of nanoscale thickness. The primer layer, significantly thicker than the pretreatment layer (up to several hundred microns), is primarily responsible for providing corrosion resistance. Finally, the topcoat serves to tailor the surface properties, such as colour, gloss, and durability, while enhancing the resistance of the overall coating system against

environmental factors, including UV radiation, mechanical impact, friction, and wear.

III. RELEVANCE OF GRAPHENE IN CORROSION PROTECTION

The application of graphene as a corrosion-resistant coating has been extensively investigated due to its impermeable lattice structure, which effectively inhibits the diffusion of corrosive species. When incorporated into metal matrices or applied as composite coatings, graphene enhances the barrier performance and electrochemical stability of the underlying substrate. Specifically, the development of nickel-graphene (Ni-Graphene) composite coatings has demonstrated promising results in improving the corrosion resistance of copper substrates, which are widely used in electrical and industrial applications.

The integration of high-quality graphene produced via sustainable synthesis methods into protective coating aligns with global efforts to mitigate the environmental footprint associated with metal degradation and corrosion protection strategies. Therefore, establishing a scalable route to synthesize defect-minimized graphene with minimal ecological consequences is of considerable scientific and technological relevance. Graphene has gained significant attention as an effective corrosion barrier due to its intrinsic impermeability and outstanding chemical resistance to aggressive species such as oxygen and water [10]. These protective attributes primarily arise from its atomically thin yet robust lattice structure, which provides remarkable mechanical strength and stability. As depicted in Fig. 3 (a), the intrinsic pore size of pristine graphene is approximately 0.064 nm, far smaller than the van der Waals diameters of

typical penetrating species, including helium 0.140 nm, hydrogen 0.120 nm, oxygen 0.152 nm, sodium 0.227 nm, and chlorine 0.175 nm [11]. This geometric constraint creates a substantial energy barrier against atomic diffusion. For instance, the calculated energy required for an oxygen atom to pass directly through the graphene lattice is around 16.34 eV, as shown in Fig. 3 (b), which is considerably higher than thermal energies at ambient conditions. Even when considering alternate reaction pathways, the energy threshold remains prohibitively high, effectively preventing the permeation of oxygen through the graphene layer [12]. This unique combination of structural compactness and energetic resistance underscores graphene's potential in anti-corrosive applications.

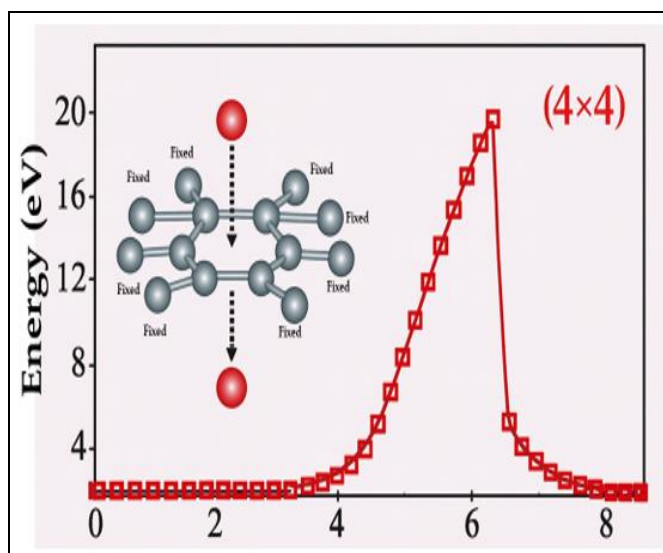
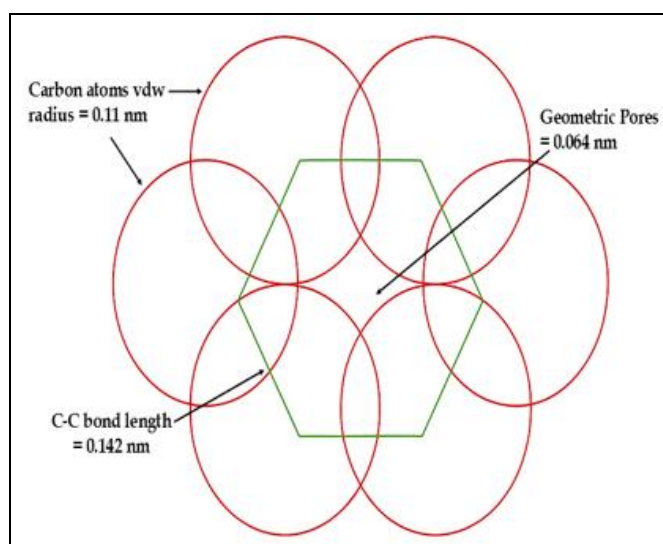


Fig 3 (a) A Conceptual Representation of the Intrinsic Pore Structure Within the Graphene Lattice, and [18] (b) the Corresponding Potential-Energy Profile that Describes the Resistance Encountered by an Oxygen Atom as it Traverses the Graphene Sheet Along a Constrained Vertical Trajectory [12].

Despite the general consensus that pristine graphene is impermeable to all atoms and molecules, recent studies have

demonstrated that monolayer graphene can allow proton transport under specific conditions [13]. As illustrated in fig. 3 (a), the atomic lattice of graphene presents an effective pore area of approximately 1.32 \AA^2 , derived from its pore diameter of around 64 pm. Protons, possessing an ionic radius as small as 0.000875 pm [14], are theoretically capable of traversing such nano-sized openings [13]. In the experimental setup by Hu et al [15] shown in fig. 3 (b), hydrogen flux was measured through a graphene membrane under an applied bias. When a negative voltage was applied to the graphene, protons originating from a PdHx electrode migrated across both Nafion and the graphene layer, producing molecular hydrogen detectable in a vacuum chamber via mass spectrometry. The experimental data (shown as scattered points) aligned well with the theoretical predictions (depicted by the red line). Notably, their finding also revealed that bilayer graphene does not permit proton transport, highlighting the critical role of atomic thickness in such phenomena. Further supporting evidence was provided by Achtyl et al. [13], who reported that protons in aqueous media use a Grothuss-type proton-hopping mechanism [16]. These insights suggest that while graphene is an effective diffusion barrier for most species, its permeability to protons, particularly in acidic environments, must be carefully considered when evaluating its performance as an anti-corrosion coating.

IV. NI-GRAPHENE ANIT-CORROSIVE COATINGS

Despite extensive advancements in graphene synthesis over the past two decades, several gaps remain in the current body of literature, particularly concerning the scalable, eco-friendly, and cost-effective production of high-quality graphene. Conventional synthesis techniques such as chemical vapor deposition (CVD), mechanical exfoliation, and chemical reduction of graphene oxide either suffer from high operational costs, harsh chemical usage, or limited scalability. While electrochemical exfoliation has recently gained attention due to its environmental compatibility and relatively mild conditions, many reported studies have utilized strong acidic or oxidizing electrolytes, leading to partial oxidation or structural defects in the graphene sheets.

Moreover, most studies focus on either high yield or structural quality, with few achieving a balance between both. The literature also shows a lack of consensus regarding optimal electrolyte composition, electrode configuration, and operational parameters such as temperature and applied voltage for defect-minimized exfoliation. There is limited work on the incorporation of green co-electrolyte such as naturally derived substances like lemon juice combined with metal salts like FeSO_4 to enhance exfoliation while simultaneously minimizing defect generation.

Additionally, relatively few studies comprehensively explore the electrochemical exfoliation process at elevated temperatures, despite evidence suggesting improved interlayer ion diffusion and defect healing under such conditions. These underexplored variables represent a critical opportunity to refine electrochemical exfoliation into a truly sustainable, high-performance synthesis method.

V. CONCLUSION

Corrosion remains an unavoidable thermodynamically driven process that continues to compromise metallic structures across industrial and domestic sectors. Although corrosion reactions are fundamentally spontaneous under most service conditions, the practical rate and severity of corrosion depend strongly on electrochemical kinetics, environmental chemistry, and microstructural heterogeneity. The thermodynamic framework based on the Second Law of Thermodynamics and standard reduction potentials provides a valuable foundation for understanding corrosion feasibility; however, effective corrosion control requires a combined consideration of kinetics, mass transport, and surface film stability. The present review has summarized major corrosion forms and has critically discussed established corrosion protection strategies, including inhibitors, cathodic protection, alloying, and coating technologies. Among emerging materials, graphene has attracted considerable attention as a corrosion-resistant barrier due to its unique two-dimensional structure, chemical inertness, and near-impermeability to gases and ions. Nevertheless, the protective capability of graphene is strongly dependent on the presence of defects, cracks, and weak interfacial bonding, which may otherwise create preferential pathways for electrolyte penetration and localized corrosion initiation. Therefore, graphene-based protection is most effective when graphene is incorporated within dense matrices or combined with metallic systems that enhance adhesion and structural compactness.

In this context, nickel–graphene composite coatings represent a promising protective platform that integrates the mechanical robustness of nickel with the barrier functionality of graphene. The reviewed studies indicate that graphene incorporation can promote grain refinement, reduce coating porosity, and increase charge-transfer resistance, thereby enhancing corrosion performance in chloride-containing environments. However, challenges remain in achieving uniform graphene dispersion, reproducible electrodeposition conditions, and long-term stability under real service conditions involving thermal cycling, mechanical stress, and prolonged immersion.

Future research should focus on controlling graphene defect density, improving coating/substrate interfacial adhesion, and developing scalable deposition routes suitable for industrial manufacturing. Additionally, advanced characterization and modeling approaches are required to establish reliable structure–property–performance correlations. Long-term exposure studies, salt spray testing, and in situ electrochemical monitoring will be essential to validate the practical durability of Ni–graphene coatings. Overall, graphene-enabled composite coatings, particularly Ni–graphene systems, are expected to play a significant role in the next generation of corrosion-resistant materials, offering a pathway toward durable, multifunctional, and environmentally sustainable protection technologies.

REFERENCES

- [1]. Standard Terminology for Corrosion, NACE Publications Style Manual, 2nd ed., (NACE International: Houston, TX, 1989).
- [2]. Ahmad, Z. Principles of corrosion engineering and corrosion control. (Butterworth Heinemann, 2006).
- [3]. Feng, L., Wu, L., Qu, X. 2013. New horizons for diagnostics and therapeutic applications of graphene and graphene oxide. *Advanced Materials* 25:168–186.
- [4]. Averill, B. A. et al. Principles of general chemistry. Creative Commons, (2012).
- [5]. Mathaudhu, S. N. et al. Essential Readings in Magnesium Technology. (Springer, 2016).
- [6]. Twite, R. et al. Review of alternatives to chromate for corrosion protection of aluminum aerospace alloys. *Prog. Org. Coat.* 33, 91-100, (1998).
- [7]. Hou, B. et al. The cost of corrosion in China. *npj Materials Degradation* 1, 4, (2017).
- [8]. Tamaki, S. et al. Advance in Corrosion Protection and Its Material. *Shinnittetsu Giho*, 2-5, (2002).
- [9]. Revie, R. W. Corrosion and corrosion control. (John Wiley & Sons, 2008).
- [10]. Su, Y. et al. Impermeable barrier films and protective coatings based on reduced graphene oxide. *Nat Commun* 5, (2014)
- [11]. Bondi, A. van der Waals Volumes and Radii. *The Journal of Physical Chemistry* 68, 441-451, (1964).
- [12]. Topsakal, M. et al. Graphene coatings: an efficient protection from oxidation. *Physical Review B* 85, 155445, (2012).
- [13]. Achtyl, J. L. et al. Aqueous proton transfer across single-layer graphene. *Nature communications* 6, (2015).
- [14]. Mohr, P. J. et al. CODATA recommended values of the fundamental physical constants: 2014. *J. Phys. Chem. Ref. Data* 45, 043102, (2016).
- [15]. Hu, S. et al. Proton transport through one-atom-thick crystals. *Nature* 516, 227-230, (2014).
- [16]. Agmon, N. The grotthuss mechanism. *Chem. Phys. Lett.* 244, 456-462, (1995).
- [17]. Cottis, R. Shreir's corrosion. (2010).
- [18]. Berry, V. Impermeability of graphene and its applications. *Carbon* 62, 1-10, (2013).